Kasula et al., http://dx.doi.org/10.1083/jcb.201508118

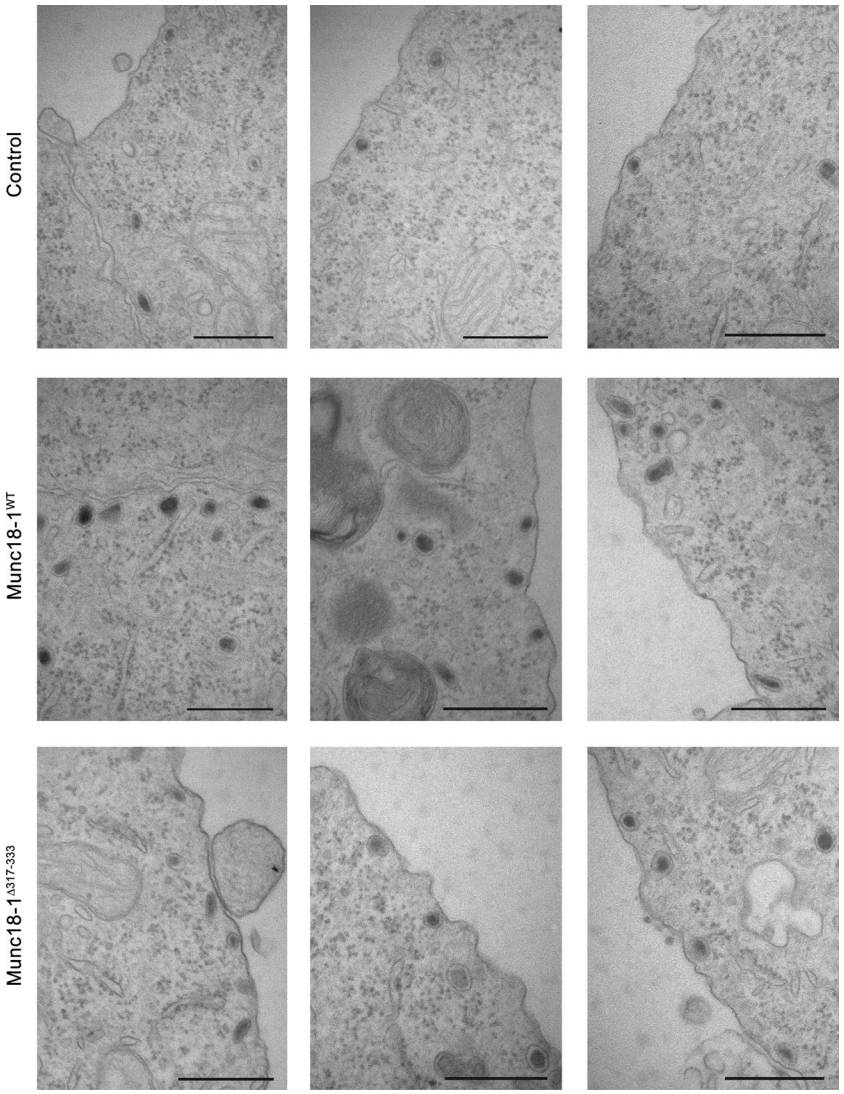

Figure S1. **Munc18-1^{WT} and Munc18-1$^{\Delta 317-333}$ rescue docking of SVs in DKD-PC12 cells.** Three representative images of DKD-PC12 cells transfected with empty pCMV, pCMV-emGFP-Munc18-1^{WT}, or pCMV-emGFP-Munc18-1$^{\Delta 317-333}$. More vesicles docked at the plasma membrane when cells were transfected with Munc18-1^{WT} or Munc18-1$^{\Delta 317-333}$. Bars, 0.5 µm.

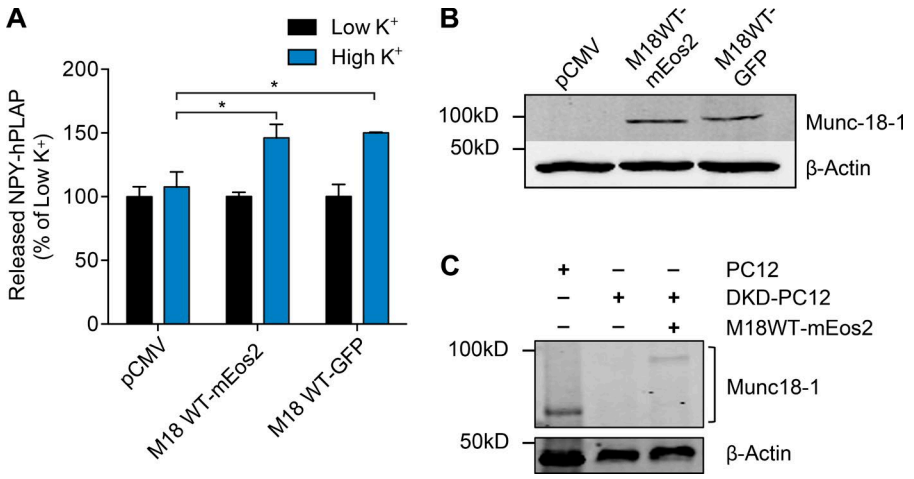

Figure S2. **Both Munc18-1^{WT}-GFP and mEos2 rescue neuroexocytosis when expressed in DKD-PC12 cells.** (A) DKD-PC12 cells were cotransfected with NPY-hPLAP and empty pCMV vector, Munc18-1^{WT}-GFP, or Munc18-1^{WT}-mEos2. Cells were treated with either low K^+ or high K^+ buffer to elicit secretion for 15 min. Released NPY-hPLAP was expressed as a percentage of low K^+ release. Results are expressed as mean ± SEM. Unpaired Student's *t* test: *, $P < 0.05$ ($n = 3–6$). (B) Transfected cells were analyzed by Western blotting of Munc18-1, and the amounts of Munc18-1^{WT}-GFP (M18WT-GFP) and Munc18-1^{WT}-mEos2 (M18WT-mEos2) were similar. Note that DKD-PC12 cells expressing pCMV alone do not contain any endogenous Munc18-1/2. β-Actin was used as a loading control. (C) Endogenous Munc18-1 levels were compared between untransfected PC12 cells and DKD-PC12 cells expressing Munc18-1^{WT}-mEos2. Only higher molecular mass Munc18-1^{WT}-mEos2 fusion protein expression is evident when reexpressed in DKD-PC12 cells.

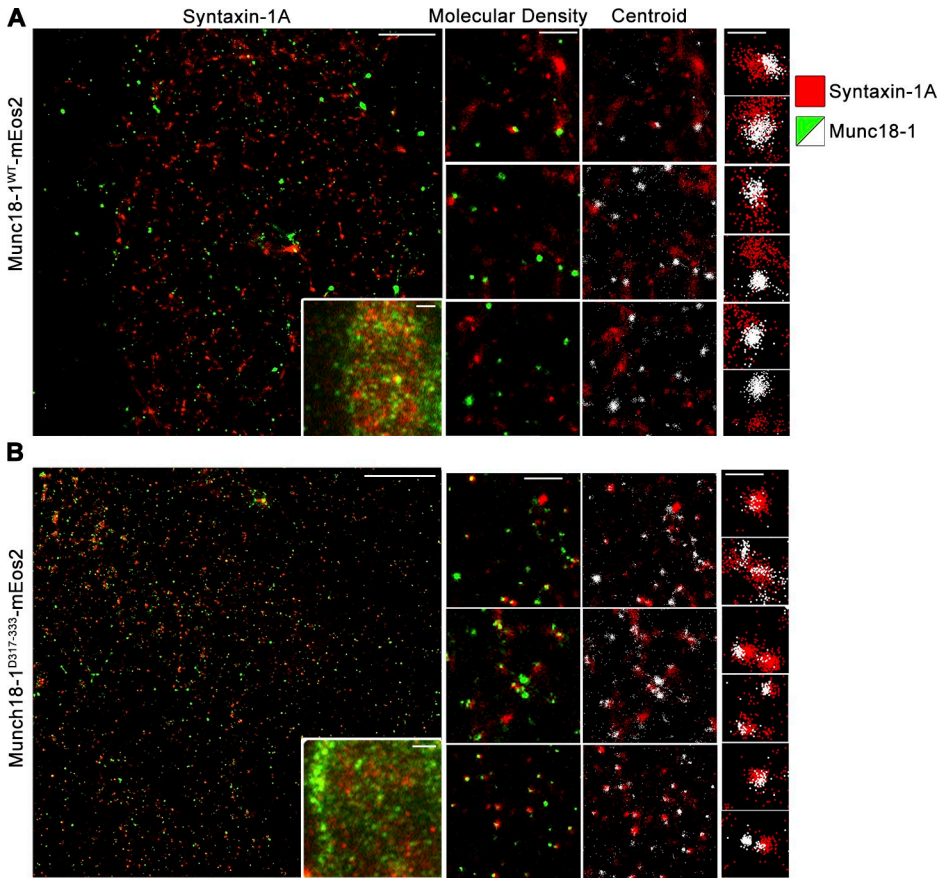

Figure S3. **Munc18-1 nanoclusters are associated with syntaxin-1A nanodomains.** DKD-PC12 cells were transfected with Munc18-1^{WT}-mEos2 (A) or Munc18-1$^{\Delta 317\text{-}333}$-mEos2 (B), fixed, and immunolabeled using an antibody against syntaxin-1A before direct stochastic optical reconstruction microscopy/PALM imaging. A representative reconstructed single-molecule localization image of a cell labeled for syntaxin-1A expressing Munc18-1^{WT}-mEos2 (A) or Munc18-1$^{\Delta 317\text{-}333}$-mEos2 (B) and a low-resolution image (inset) are shown. The middle panels depict molecule density and the centroids of individual localizations. Bars, 1 µm. The right panels show further enlargements of clusters containing Munc18-1 and syntaxin-1A from these images. Bars, 300 nm.

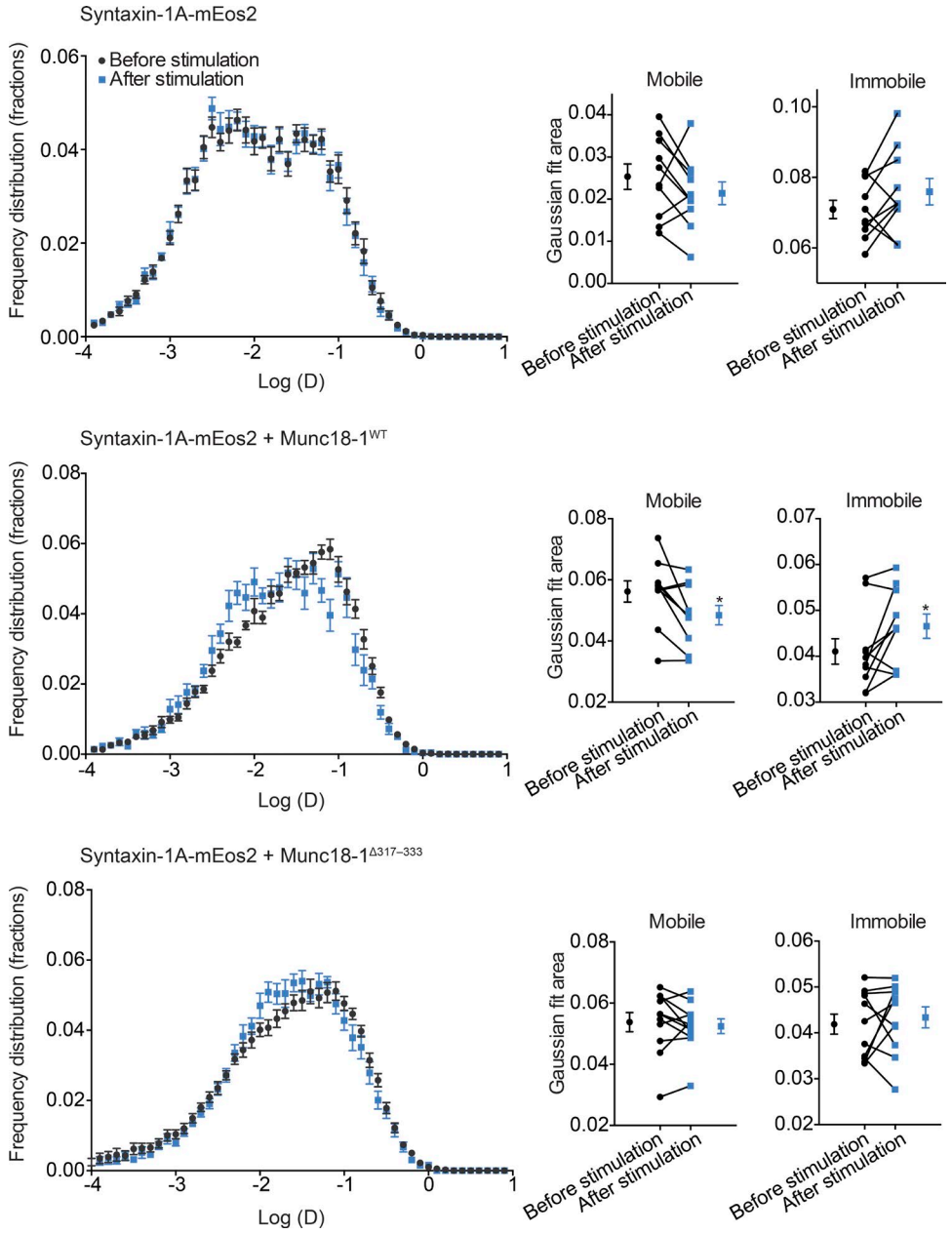

Figure S4. **Munc18-1 3a domain loop controls the activity-dependent decrease in syntaxin-1A mobility.** DKD-PC12 cells expressing syntaxin-1A-mEos2 either alone or with untagged Munc18-1^{WT} or Munc18-1$^{\Delta 317\text{-}333}$ were imaged at 20 Hz for 10 min before stimulation and 5 min after stimulation (2 mM Ba^{2+}) using the sptPALM technique with Marianas TIRF imaging for the same cell. At left, mean distribution of the diffusion coefficient and comparison before and after stimulation of the area under the curve of the mobile (middle) and immobile (right) fractions. The area under the curve was derived from a binary Gaussian fit of the histograms of the diffusion coefficients using Matlab (n = 10–15 cells for each condition; paired Student's t test, *, $P < 0.05$). Error bars show SEM.

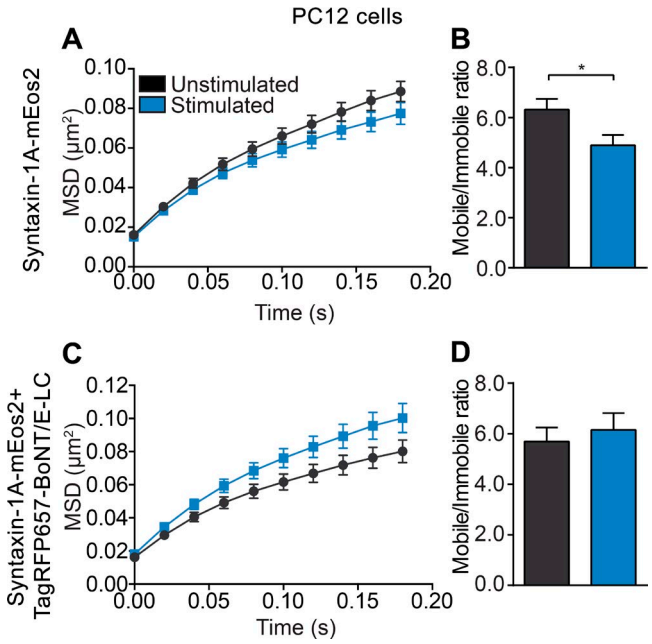

Figure S5. **BoNT/E-LC expression prevents the activity-dependent decrease in syntaxin-1A mobility.** PC12 cells expressing syntaxin-1A-mEos2 either alone or with TagRFP657-BoNT/E-LC were imaged at 50 Hz in unstimulated or stimulated (2 mM Ba^{2+}) conditions using sptPALM. (A–D) MSDs of single-molecule trajectories are shown as a function of time, and the ratio of the mobile to immobile fraction in indicated cells and conditions is illustrated (n = 13–23 cells for each condition; Mann-Whitney U test for MSDs and unpaired Student's t test for the rest; *, $P < 0.05$). Error bars show SEM.